Available online at www.sciencedirect.com
ScienceDirect
Engineering Fracture Mechanics 75 (2008) 1829–1839
Engineering Fracture Mechanics
www.elsevier.com/locate/engfracmech

# Application of the point stress criterion to the failure of composite pinned joints ☆

H.A. Whitworth *, O. Aluko, N.A. Tomlinson

*Department of Mechanical Engineering, College of Engineering, Architecture and Computer Sciences, Howard University, 2300 Sixth Street, NW, Washington, DC 20059, United States*

Received 29 July 2006; received in revised form 2 December 2006; accepted 4 December 2006
Available online 25 January 2007

**Abstract**

An analysis was performed to evaluate the bearing strength of pin-loaded composite joints using a two parameter characteristic curve model. This model involves determination of characteristic dimensions in tension and compression and based on this model, a two-dimensional stress analysis was used to determine the stress distribution around the fastener hole. In this analysis, characteristic dimensions in tension and compression were evaluated using the point stress failure criterion and joint bearing failure evaluated using the Yamada–Sun failure criterion. Results were compared with available experimental data for joints made from AS4/3501-6 graphite epoxy composite laminates and good correlation observed when evaluated as function of edge distance to hole diameter. However, the analysis yields conservative results when joint strength is evaluated as a function of plate width to hole diameter.


*Keywords:* Composites; Fiber reinforced materials; Pinned joints; Failure assessment

## 1. Introduction

Joints are necessary load transfer elements of components or structures and the performance of these structures or components is critically dependent upon the behavior of any joints they contain. Joining by mechanical fasteners is a common practice in the assembly of structures and since joint failure can lead to premature failure of the structure, joint strength is an important property in any design. Mechanical joining requires rivets and/or bolts through holes which result in stress concentrations that may ultimately lead to failure. Adhesive joints, on the other hand, do not require holes and distribute the load over a larger area than mechanical

☆ This article appeared in its original form in *Fracture of Nano and Engineering Structures: Proceedings of the 16th European Conference of Fracture, Alexandroupolis, Greece, July 3–7, 2006* (Edited by E.E. Gdoutos, 2006). Springer, Dordrecht, The Netherlands. ISBN 1-4020-4971-4.

* Corresponding author. Tel.: +1 202 806 6600; fax: +1 202 483 1396.
*E-mail address:* hwhitworth@howard.edu (H.A. Whitworth).

0013-7944/$ - see front matter © 2006 Elsevier Ltd. All rights reserved.
doi:10.1016/j.engfracmech.2006.12.003

**Nomenclature**

| | |
|---|---|
| $A, B$ | normal stresses in the reinforcement |
| $\overline{A}, \overline{B}$ | normalized stresses in the inclusion |
| $A^*, B^*$ | parameters dependent on laminate properties |
| $D$ | hole diameter |
| $D^*$ | parameter dependent on laminate properties |
| $E$ | distance from laminate edge to hole center |
| $E_1, E_2, G_{12}, E_x, E_y, G_{xy}$ | elastic modulus |
| $K_T, K_T^\infty$ | stress concentration factors for finite and infinite plates |
| $L$ | plate length |
| $P$ | applied uniform stress at infinity |
| $p_k, q_k$ | parameters dependent on laminate properties |
| $r_c$ | characteristic curve model |
| $R$ | hole radius |
| $R_t, R_c$ | characteristic dimension in tension and compression |
| $s$ | shear failure mode |
| $S$ | lamina shear strength |
| $\overline{S}_{ij}$ | elastic compliance |
| $t$ | tension failure mode |
| $T$ | plate thickness |
| $u, v$ | displacements in $x$ and $y$ directions |
| $v_0$ | pin displacement along $y$-direction |
| $W$ | plate width |
| $X_T, X_C, Y_T, Y_C$ | lamina strengths in tension and compression |
| $Y$ | finite width correction factor |
| $\sigma_x, \sigma_y$ | stresses in $x$ and $y$ direction |
| $\tau_{xy}$ | shear stress |
| $\sigma_N, \sigma_N^\infty$ | notch strength for finite and infinite plate |
| $\sigma_{N_C}$ | compressive strength of laminate with inclusion |
| $\sigma_F$ | unnotched laminate tensile strength |
| $\sigma_{F_C}$ | unnotched laminate compressive strength |
| $\mu_k$ | roots of characteristic equation |
| $v_{12}, v_{xy}$ | Poisson's ratio |
| $\Phi_k, \Phi_k'$ | stress function and its derivative ($k = 1, 2$) |
| $\lambda$ | coefficient of friction |
| $\tau_{12}$ | lamina shear stress |
| $\zeta_k$ | mapping function |

joints [1]. However, they are very sensitive to surface treatment, service temperature, humidity, and other environmental conditions [2]. On the other hand, for structural components that must be removed or easily replaced, mechanical fasteners play an important role.

The increased use of advanced composite materials for structural applications has led to extensive research aimed at developing an understanding of the behavior of these structures to the presence of holes and inclusions. Accurate and proper design of mechanically fastened joints require the determination of the stress distribution at the contact surface and within the plate followed by the use of an appropriate failure theory to determine the strength of the joint. The method of complex functions developed by Muskhelishvili and extended to anisotropic materials by Lekhnitskii [3] and Savin [4] has been used by several investigators [5–14] to obtain stress distribution in composite plates weakened by an opening and deformed by forces applied to the mid plane.

The present analysis of the bearing strength of pin-loaded composite joints involves using the Chang–Scott–Springer characteristic curve model and a two-dimensional analysis to evaluate the stress distribution around the fastener hole. Calculations are based on the analytical method of complex stress functions and on expressions used to satisfy the displacement boundary conditions of the contact area between the pin and the hole [10]. For the characteristic curve, characteristic dimensions in tension and compression were evaluated by applying the point stress failure criterion to a center notch plate subjected to tensile loading and a plate containing a circular inclusion subjected to compressive loading. The Yamada–Sun failure criterion [15] was then used to evaluate joint failure and the results compared with available experimental data and good correlation observed.

## 2. Stress analysis

In order to evaluate the strength of composite pinned joints (Fig. 1), the stress distribution along a characteristic dimension around the hole must first be evaluated. The conditions for failure can then be predicted with the aid of an appropriate failure criterion. The Yamada–Sun failure criterion was used for this analysis. This criterion is given by the relationship [15]

$$\left(\frac{\sigma_1}{X}\right)^2 + \left(\frac{\tau_{12}}{S}\right)^2 = e^2 \tag{1}$$

where $\sigma_1$ and $\tau_{12}$ are the longitudinal and shear stresses, $X$ is the ply longitudinal strength and $S$ is the ply shear strength. In this model, failure is expected to occur when the value of $e$ is greater than or equal to unity.

The characteristic curve model proposed by Chang et al. [8] can be expressed as

$$r_c(\theta) = R + R_t + (R_c - R_t)\cos\theta \tag{2}$$

where $R$ is the hole radius, $R_t$ and $R_c$ the characteristic dimensions in tension and compression, and the angle $\theta$ ranges in value from $-\pi/2$ to $\pi/2$ (Fig. 2). The parameters $R_t$ and $R_c$ were evaluated by applying the point stress failure criterion to a plate with an open hole loaded in tension and a plate with an inclusion loaded in compression [9].

Konish and Whitney [13] proposed the following approximate solution for the normal stress distribution $\sigma_y(x,0)$ in an infinite orthotropic plate with an open hole loaded in tension by a uniform stress $P$ at infinity

$$\frac{\sigma_y(x,0)}{P} \cong 1 + \frac{1}{2}\xi^{-2} + \frac{3}{2}\xi^{-4} - \frac{(K_T^\infty - 3)}{2}(5\xi^{-6} - 7\xi^{-8}) \tag{3}$$

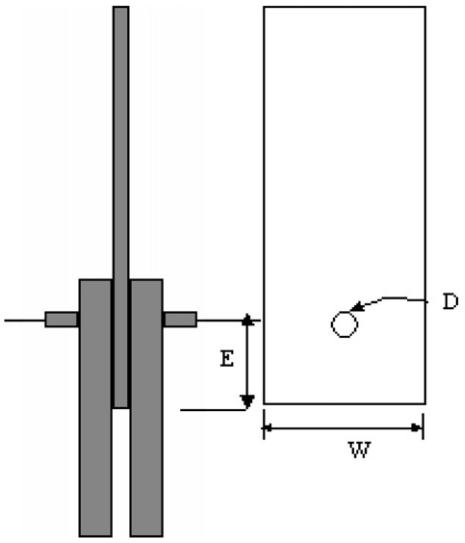


Fig. 1. Geometry of composite pin joint.

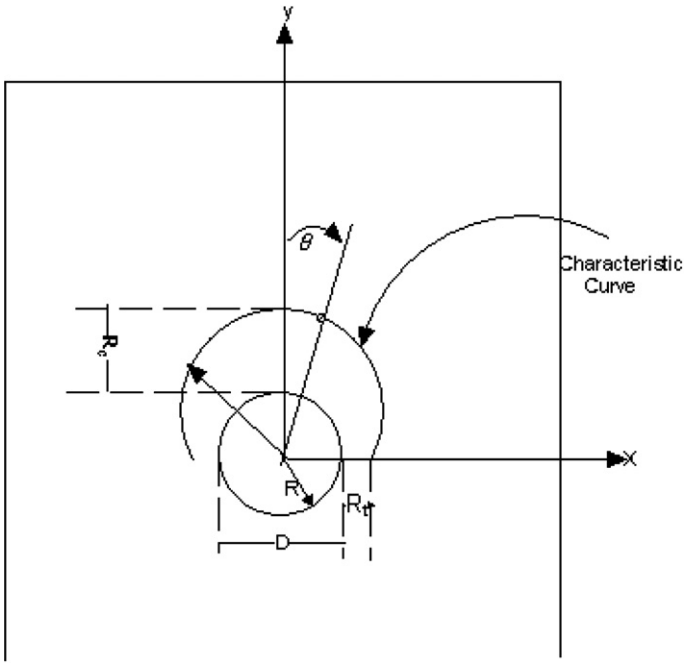


Fig. 2. Composite plate with characteristic curve description.

where

$$\xi = \frac{x}{R} \tag{4}$$

and $K_T^\infty$ is the orthotropic stress concentration factor defined as

$$K_T^\infty = 1 + \sqrt{\frac{2}{\overline{S}_{22}}\left(\sqrt{(\overline{S}_{11}\overline{S}_{22})} - \overline{S}_{12} + \frac{(\overline{S}_{11}\overline{S}_{22} - \overline{S}_{12}^2)}{2\overline{S}_{66}}\right)} \tag{5}$$

The point stress failure criterion can be applied to Eq. (3) to determine the characteristic dimension at which failure is expected to occur. This criterion assumes that failure occurs when the transverse stress at some distance $R_t$ away from the opening reaches the unnotched tensile strength, $\sigma_F$, of the material. This criterion is expressed as

$$\sigma_y(R + R_t, 0) = \sigma_F \tag{6}$$

Substituting Eq. (6) into Eq. (3), the ratio of the notched to the unnotched strength is obtained as

$$\frac{\sigma_N^\infty}{\sigma_F} = \frac{2}{2 + \xi^{-2} + 3\xi^{-4} - (K_T^\infty - 3)(5\xi^{-6} - 7\xi^{-8})} \tag{7}$$

where $\sigma_N^\infty$ is the tensile strength of the notched laminate and, at $x = R + R_t$,

$$\xi = \frac{R + R_t}{R} \tag{8}$$

Eq. (7) contains two unknown parameters, the unnotched laminate tensile strength $\sigma_F$ and the characteristic length $R_t$. A value of $R_t$ for a laminate can be determined from Eq. (7), if the experimental data for both the notched and unnotched strengths are available or by applying classical lamination theory in conjunction with an appropriate lamina failure criterion to evaluate these parameters.

Eq. (7) represents the stress reduction factor for an infinite plate. In order to apply this relation to plates of finite width, finite width correction factors must be applied. The finite width correction factor (FWC) can be expressed as [16]

$$\frac{K_T}{K_T^\infty}\sigma_N^\infty = \sigma_N \tag{9}$$

where $K_T$ and $K_T^\infty$ denote the stress concentration at the opening edge on the axis normal to the applied load for a finite plate and an infinite plate respectively. However, it should be noted that since tensile failure occurs at $x = R + R_t$, Eq. (9) represents an approximate relation between $K_T/K_T^\infty$ and $\sigma_N/\sigma_N^\infty$.

For composite plates with a circular opening, Tan [16] has shown that the FWC factor can be expressed as

$$\frac{K_T}{K_T^\infty} = Y = \frac{\left[2 - (\frac{D}{W})^2 - (\frac{D}{W})^4\right]}{2} + \frac{\left[(\frac{D}{W})^6(K_T^\infty - 3)(1 - (\frac{D}{W})^2)\right]}{2} \tag{10}$$

where $D$ is the hole diameter and $W$ is the plate width. From Eqs. (9) and (10), the notched strength for a finite laminate can be obtained from the notch strength determined for an infinite plate as

$$\sigma_N = Y\sigma_N^\infty \tag{11}$$

As stated previously, in order to evaluate failure of mechanically fastened joints based on the characteristic curve model, the characteristic length in compression must also be evaluated. This value is obtained from evaluation of the stress distribution in a plate with an inclusion subjected to compressive loading.

The normal stress $\sigma_y(x,0)$ for an infinite orthotropic plate with an inclusion under uniform stress $P$ at infinity can be expressed as [3]

$$\frac{\sigma_y(x,0)}{P} = 1 + \mathrm{Re}\left\{\frac{1}{\mu_1 - \mu_2}\left[\frac{-(1-\overline{B})(\mu_1 - i\mu_1\mu_2) - (i+\mu_1)\overline{A}}{\psi_1} + \frac{(1-\overline{B})(\mu_1 - i\mu_1\mu_2) + (i+\mu_2)\overline{A}}{\psi_2}\right]\right\} \tag{12}$$

where $\mu_i$ $(i = 1,2)$ are the roots of characteristics equation

$$\overline{S}_{11}\mu^4 + 2(\overline{S}_{12} + \overline{S}_{66})\mu^2 + \overline{S}_{22} = 0 \tag{13}$$

and

$$\psi_k = \frac{1}{\sqrt{(\xi^2 - 1 - \mu_k^2)}\left(\xi + \sqrt{\xi^2 - 1 - \mu_k^2}\right)}, \quad k = 1,2 \tag{14}$$

In Eq. (12), $\overline{A}$ and $\overline{B}$ can be obtained from the following relations:

$$\begin{aligned}\overline{A} &= \frac{A}{P} = \frac{1}{\Delta}\left[\overline{S}_{11}\overline{S}_{22}(k+n) + \overline{S}_{11}\overline{S'}_{22}k(1+n) + \overline{S}_{22}(\overline{S}_{12} + \overline{S}_{66} + \overline{S'}_{12})\right]\\ \overline{B} &= \frac{B}{P} = \frac{1}{\Delta}\left[\overline{S}_{22}(\overline{S}_{11} - \overline{S'}_{11}) + \overline{S}_{11}(\overline{S}_{12} - \overline{S'}_{12})k(1+n)\right]\end{aligned} \tag{15}$$

where $A$ and $B$ denote the normal stresses in the reinforcement along the $x$ and $y$ axis, the primed quantities denote the elastic constants for the inclusion,

$$\Delta = (\overline{S}_{11}\overline{S}_{22} + \overline{S}'_{11}\overline{S}'_{22})k + \overline{S}_{22}(\overline{S}_{66} + 2\overline{S}_{12}) + (\overline{S}_{11}\overline{S}'_{22}k + \overline{S}_{22}\overline{S}'_{11})n - (\overline{S}_{12} - \overline{S}'_{12})^2 k \tag{16}$$

and

$$k = -\mu_1\mu_2 \quad \text{and} \quad n = -i(\mu_1 + \mu_2) \tag{17}$$

Eq. (12) is the solution for the stress distribution adjacent to the inclusion in an infinite orthotropic plate with a filled circular cavity. In order to apply the point stress criterion to determine $R_c$, a symbolic computer code was written using Mathematica to determine the real part of this equation [9]. From this analysis, the real part of Eq. (12) is expressed as

$$\frac{\sigma_y(x,0)}{P} = 1 + \left(\frac{\Psi_{11} + \Psi_{12} + \Psi_{21} + \Psi_{22}}{\Delta_T}\right) \tag{18}$$

where

$$\begin{aligned}
\Psi_{11} &= -\overline{A}\beta^2 + (\overline{B}-1)\beta^3 + \overline{A}\alpha^2(1+\beta) - (\overline{B}-1)(1+\beta)\alpha^3 + \overline{A}\xi\left(\sqrt{\xi^2-1+\alpha^2} - \sqrt{\xi^2-1+\beta^2}\right)\\
\Psi_{12} &= \beta\left(1-\overline{A}-\overline{B}-\xi^2+\overline{A}\xi^2+\overline{B}\xi^2+\overline{A}\xi\sqrt{\xi^2-1+\alpha^2} - (1-\overline{B})\xi\sqrt{\xi^2-1+\beta^2}\right)\\
\Psi_{21} &= -\alpha\overline{A}\left(\xi^2-1+\beta^2+\xi\sqrt{\xi^2-1+\beta^2}\right)\\
\Psi_{22} &= \alpha(\overline{B}-1)\left(1-\xi^2+\beta^3-(\beta+1)\xi\sqrt{\xi^2-1+\alpha^2}+\beta\xi\sqrt{\xi^2-1+\beta^2}\right)\\
\Delta_{\mathrm{T}} &= (\alpha-\beta)\left[\sqrt{\xi^2-1+\alpha^2}\sqrt{\xi^2-1+\beta^2}\left(\xi+\sqrt{\xi^2-1+\alpha^2}\right)\left(\xi^2\sqrt{\xi^2-1+\beta^2}\right)\right]
\end{aligned} \tag{19}$$

and

$$\begin{aligned}
\alpha &= \frac{1}{2}\left\{\sqrt{\frac{E_x}{G_{xy}} - 2\nu_{xy} + 2\sqrt{\frac{E_x}{E_y}}} + \sqrt{\frac{E_x}{G_{xy}} - 2\nu_{xy} - \sqrt{\frac{E_x}{E_y}}}\right\}\\
\beta &= \frac{1}{2}\left\{\sqrt{\frac{E_x}{G_{xy}} - 2\nu_{xy} + 2\sqrt{\frac{E_x}{E_y}}} - \sqrt{\frac{E_x}{G_{xy}} - 2\nu_{xy} - \sqrt{\frac{E_x}{E_y}}}\right\}
\end{aligned} \tag{20}$$

The point stress criterion can then be applied to obtain $R_{\mathrm{c}}$, the characteristic length in compression. This criterion is expressed as

$$\sigma_y(R+R_{\mathrm{c}},0) = \sigma_{\mathrm{F_C}} \tag{21}$$

and substitution of Eq. (21) into Eq. (18) gives

$$\frac{\sigma^{\infty}_{\mathrm{N_C}}}{\sigma_{\mathrm{F_C}}} = \frac{1}{\left[1+\left(\frac{\Psi_{11}+\Psi_{12}+\Psi_{21}+\Psi_{22}}{\Delta_{\mathrm{T}}}\right)\right]} \tag{22}$$

where $\sigma_{\mathrm{F_C}}$ is the compressive strength of the unnotched laminate, $\sigma^{\infty}_{\mathrm{N_C}}$ the compressive strength of the notched laminate with inclusion and, at $x = R + R_{\mathrm{c}}$,

$$\xi = \frac{R+R_{\mathrm{C}}}{R} \tag{23}$$

A value of $R_{\mathrm{c}}$ for a laminate can be determined from Eq. (22), if the experimental data on the unnotched compressive strength of the plate and the compressive strength of the notched plate with an inclusion are available. If experimental data is not available, these values can be obtained by applying classical lamination theory in conjunction with an appropriate lamina failure criterion [12].

## 3. Strength prediction

Consider an infinite plate with a circular opening subjected to pin load $F_{\mathrm{P}}$, as shown in Fig. 3. As seen in this figure, the hole boundary can be described by contact and no contact regions. In this analysis, the pin is assumed to be rigid and of the same diameter as the hole. Additionally, slip is assumed to occur throughout the contact region and coulomb friction chosen to evaluate the condition of friction between the pin and the hole.

The stresses in the plate can be expressed as [3]

$$\begin{aligned}
\sigma_x &= 2\mathrm{Re}\left(\mu_1^2\Phi_1'(z_1) + \mu_2^2\Phi_2'(z_2)\right)\\
\sigma_y &= 2\mathrm{Re}\left(\Phi_1'(z_1) + \Phi_2'(z_2)\right)\\
\tau_{xy} &= -2\mathrm{Re}\left(\mu_1\Phi_1'(z_1) + \mu_2\Phi_2'(z_2)\right)
\end{aligned} \tag{24}$$

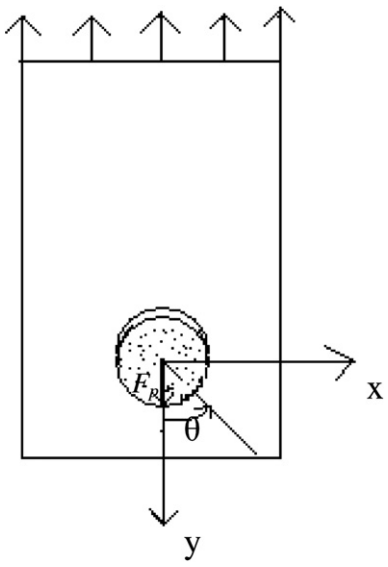


Fig. 3. Schematic representation of a pin loaded plate.

Let the displacement of the pin along the $y$-axis due to the applied load be denoted by $v_0$. The boundary conditions within the contact region for this problem can be expressed as

$$v = v_0/c \quad \text{and} \quad u = 0 \quad \theta = \pm\frac{\pi}{2} \tag{25}$$

$$v = v_0 \quad \text{and} \quad u = 0 \quad \theta = 0 \tag{26}$$

$$(v_0 - v)\cos\theta = u\sin\theta \quad -\frac{\pi}{2} \leqslant \theta \leqslant \frac{\pi}{2} \tag{27}$$

where $u$ and $v$ are the displacement along $x$ and $y$ directions, respectively, and $c$ is a constant.

Additionally, at the contact boundary $\theta = \pm\pi/2$

$$\begin{aligned} \sigma_x &= 0 \\ \tau_{xy} &= 0 \end{aligned} \tag{28}$$

The displacements $u$ and $v$ along the hole can be expressed by the following trigonometric series

$$\begin{aligned} u &= U_1\sin 2\theta + U_2\sin 4\theta \\ v &= V_1\cos 2\theta + V_2\cos 4\theta \end{aligned} \tag{29}$$

where $U_i$ and $V_i$ $(i = 1, 2)$ are constants to be determined from the boundary conditions.

For the case where the plate is loaded by a rigid pin which has the same diameter as the hole, the stress functions can be expressed as [10]

$$\Phi_1(z_1) = A^*\ln\zeta_1 + \left(\frac{c-1}{2c}\frac{q_2 - ip_2}{2D^*} - \frac{c+1}{c}\frac{ip_2}{2D^*}\right)\frac{v_0}{\zeta_1^2} + \frac{c+1}{2c}\frac{q_2 - ip_2}{2D^*}\frac{v_0}{\zeta_1^4} \tag{30}$$

$$\Phi_2(z_2) = B^*\ln\zeta_2 + \left(-\frac{c-1}{2c}\frac{q_1 - ip_1}{2D^*} - \frac{c+1}{c}\frac{ip_1}{2D^*}\right)\frac{v_0}{\zeta_2^2} - \frac{c+1}{2c}\frac{q_1 - ip_1}{2D^*}\frac{v_0}{\zeta_2^4} \tag{31}$$

where $A^*$, $B^*$, $D^*$, $p_k$ and $q_k$ are constants that depend on the material properties and complex roots $\mu_1$ and $\mu_2$ of the characteristic equation,

$$\zeta_k = \frac{z_k + \sqrt{z_k^2 - R^2(1+\mu_k^2)}}{R(1 - i\mu_k)} \tag{32}$$

and

$$z_k = x + \mu_k y, \quad k = 1, 2 \tag{33}$$

Substituting the derivatives of Eqs. (30) and (31) into Eq. (24) results in the following relations for the stresses in the plate

$$\sigma_x = 2\mathrm{Re}\left\{\left[\frac{A^*}{\zeta_1} - 2\left(\frac{c-1}{2c}\frac{q_2 - ip_2}{2D^*} - \frac{c+1}{c}\frac{ip_2}{2D^*}\right)\frac{v_0}{\zeta_1^3} - 4\left(\frac{c+1}{2c}\frac{q_2 - ip_2}{2D^*}\right)\frac{v_0}{\zeta_1^5}\right]A_1\mu_1^2 + \left[\frac{B^*}{\zeta_2} - 2\left(-\frac{c-1}{2c}\frac{q_1 - ip_1}{2D^*} + \frac{c+1}{c}\frac{ip_1}{2D^*}\right)\frac{v_0}{\zeta_2^3} + 4\left(\frac{c+1}{2c}\frac{q_1 - ip_1}{2D^*}\right)\frac{v_0}{\zeta_2^5}\right]A_2\mu_2^2\right\} \tag{34}$$

$$\sigma_y = 2\mathrm{Re}\left\{\left[\frac{A^*}{\zeta_1} - 2\left(\frac{c-1}{2c}\frac{q_2 - ip_2}{2D^*} - \frac{c+1}{c}\frac{ip_2}{2D^*}\right)\frac{v_0}{\zeta_1^3} - 4\left(\frac{c+1}{2c}\frac{q_2 - ip_2}{2D^*}\right)\frac{v_0}{\zeta_1^5}\right]A_1 + \left[\frac{B^*}{\zeta_2} - 2\left(-\frac{c-1}{2c}\frac{q_1 - ip_1}{2D^*} + \frac{c+1}{c}\frac{ip_1}{2D^*}\right)\frac{v_0}{\zeta_2^3} + 4\left(\frac{c+1}{2c}\frac{q_1 - ip_1}{2D^*}\right)\frac{v_0}{\zeta_2^5}\right]A_2\right\} \tag{35}$$

$$\tau_{xy} = -2\mathrm{Re}\left\{\left[\frac{A^*}{\zeta_1} - 2\left(\frac{c-1}{2c}\frac{q_2 - ip_2}{2D^*} - \frac{c+1}{c}\frac{ip_2}{2D^*}\right)\frac{v_0}{\zeta_1^3} - 4\left(\frac{c+1}{2c}\frac{q_2 - ip_2}{2D^*}\right)\frac{v_0}{\zeta_1^5}\right]A_1\mu_1 + \left[\frac{B^*}{\zeta_2} - 2\left(-\frac{c-1}{2c}\frac{q_1 - ip_1}{2D^*} + \frac{c+1}{c}\frac{ip_1}{2D^*}\right)\frac{v_0}{\zeta_2^3} + 4\left(\frac{c+1}{2c}\frac{q_1 - ip_1}{2D^*}\right)\frac{v_0}{\zeta_2^5}\right]A_2\mu_2\right\} \tag{36}$$

where

$$A_k = \frac{\zeta_k}{\sqrt{z_k^2 - R^2(1 - \mu_k^2)}}, \quad k = 1, 2 \tag{37}$$

Since it is desired to determine the stresses along the hole contour, Eqs. (34)–(36) can be transformed to polar coordinates through the following relations

$$\begin{aligned}
\sigma_r &= \sigma_x \cos^2\theta + \sigma_y \sin^2\theta + 2\tau_{xy}\cos\theta\sin\theta \\
\sigma_\theta &= \sigma_x \sin^2\theta + \sigma_y \cos^2\theta - 2\tau_{xy}\cos\theta\sin\theta \\
\tau_{r\theta} &= (\sigma_y - \sigma_x)\cos\theta\sin\theta + \tau_{xy}\cos^2\theta - \tau_{xy}\sin^2\theta
\end{aligned} \tag{38}$$

where $\sigma_r$, $\sigma_\theta$, and $\tau_{r\theta}$ are the transformed radial, tangential and the shear stresses, respectively. Additionally, in Eqs. (34)–(36), the parameters $v_0$ and $c$ can be determined from the material properties of the plate and the effects of friction between pin and plate. The friction condition can be expressed as

Table 1
Material properties for AS4/3501-6 laminates

| | |
|---|---|
| $E_1$ (GPa) | 144.14 |
| $E_2$ (GPa) | 11.72 |
| $G_{12}$ (GPa) | 6.69 |
| $v_{12}$ | 0.33 |
| $X_T$ (GPa) | 1.86 |
| $X_C$ (GPa) | 1.48 |
| $Y_T$ (GPa) | 0.05 |
| $Y_C$ (GPa) | 0.21 |
| $S$ (GPa) | 0.06 |
| $R_t$ (cm) | 0.09 |
| $R_c$ (cm) | 0.13 |

$$\int_0^{\pi/2} \tau_{r\theta} R \, d\theta = -\lambda \int_0^{\pi/2} \sigma_r R \, d\theta \tag{39}$$

where the frictional coefficient $\lambda$ is assumed constant along the contact boundary.

To determine the stress distribution along the characteristic curve, $x$ and $y$ in Eq. (33) are replaced by $r_c \sin\theta$ and $r_c \cos\theta$, respectively and a program written using Matlab to determine the real parts of Eqs. (34)–(36). Once the laminate stresses are calculated from Eqs. (34)–(36), classical laminate plate theory can then be used to compute the lamina stresses and the Yamada–Sun failure theory used to evaluate joint failure load and failure mode. Material properties for AS4/3501-6 graphite/epoxy laminates, summarized in Table 1, were used for this analysis. Also shown in Table 1 are the values of $R_t$ and $R_c$ obtained from Ref. [9]. Results generated from this analysis were compared with available experimental data for composite pinned joints made from AS4/3501-6 graphite/epoxy laminates utilizing steel pins [17]. The experimental results of Ref. [17] are summarized

Table 2
Experimental and predicted bearing strengths and failure modes for pin-loaded AS4/3501-6 $[(45/0/-45/0/90/0/45/0/-45/0)_2]_s$ laminates with varying $E/D$ ratios [17]

| $E/D$ | Experimental bearing strengths (MPa) | Predicted bearing strengths (MPa) | Experimental failure modes | Predicted failure modes |
|---|---|---|---|---|
| $D = 0.635$ cm, $L = 15.24$ cm, $T = 0.584$ cm | | | | |
| 1 | 320 | 402 | s | s |
| 1.5 | 600 | 712 | s | b/s |
| 2 | 802 | 772 | b/s | b |
| 3 | 900 | 825 | b | b |
| 4 | 990 | 888 | b | b |
| 5 | 980 | 840 | – | b |

Table 3
Experimental and predicted bearing strengths and failure modes for pin-loaded AS4/3501-6 $[(45/0/-45/0/90/0/45/0/-45/0)_2]_s$ laminates [16] with varying $W/D$ ratios [17]

| $W/D$ | Experimental bearing strengths (MPa) | Predicted bearing strengths (MPa) | Experimental failure modes | Predicted failure modes |
|---|---|---|---|---|
| $D = 0.635$ cm, $L = 15.24$ cm, $T = 0.584$ cm | | | | |
| 2 | 680 | 672 | t | b |
| 3 | 945 | 749 | b | b |
| 4 | 986 | 771 | b | b |
| 5 | 976 | 781 | b | b |

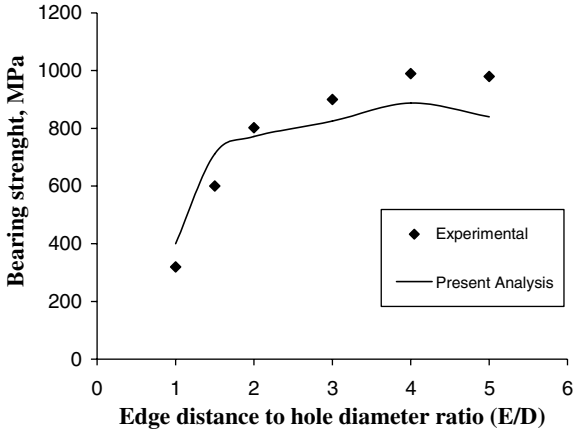


Fig. 4. Comparison between predicted results and experimental data as a function of edge to diameter ratio.

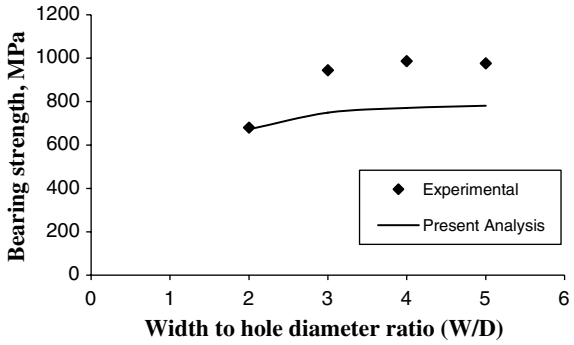


Fig. 5. Comparison between predicted results and experimental data as a function of plate width to hole diameter ratio.

in Tables 2 and 3 and, along with the results generated from the present analysis, displayed in Figs. 4 and 5. In Tables 2 and 3, b (bearing), s (shear) and t (tension) refer to the modes of failure while $D$, $L$, $W$ and $T$ refer to the diameter, length, width and thickness of the plate, respectively. Fig. 4 compares the prediction of the present analysis to experimental data as a function of edge distance to hole diameter ($E/D$) while Fig. 5 compares the prediction as a function of plate width to hole diameter ($W/D$). As shown in these figures, the present analysis gives conservative results when evaluated as a function of plate width to hole diameter while good agreement is observed when evaluated as function of edge distance to hole diameter.

## 4. Conclusions

An analysis was performed to evaluate failure of pin loaded composite joints using a two dimensional stress analysis to evaluate the stress distribution along a characteristic dimension around the hole. The characteristic dimensions were obtained using the point stress criterion in conjunction with the Chang–Scott–Springer characteristic curve model and the Yamada–Sun failure criterion used to predict failure loads and failure modes. Available experimental data for AS4/3501-6 graphite/epoxy laminates was utilized to evaluate joint bearing strength. Bearing strength was evaluated as a function of plate width to hole diameter ($W/D$) and edge distance to hole diameter ($E/D$). From the present analysis:

1. Good agreement is observed with experimental data for the graphite/epoxy laminates when the bearing strength is evaluated as function of edge distance to hole diameter. However, when evaluated as a function of plate width to hole diameter, the analysis gives conservative results.
2. In addition to the prediction of bearing strength, the proposed analysis was also used to predict failure mode using the Yamada–Sun failure theory. Again, the analysis shows good agreement with experimental data in the prediction of the failure mode for the edge distance to hole diameter analysis. Good agreement is also observed for the plate width to hole diameter analysis.

## References

[1] Choi J, Chun Y. Failure load prediction of mechanically fastened composite joints. J Compos Mater 2003;37(May):2163–216.
[2] Choi JH, Lee DG. An experimental study of the static torque capacity of the adhesively-bonded tubular single lap joint. J Adhesion 1996;55:245–60.
[3] Lekhnitskii SG. Anisotropic plates, English ed. (Tsai SW, Cheron T). London, Gordon and Beach; 1968.
[4] Savin GN. Stress concentration around holes. New York: Pergamon Press; 1968.
[5] Madenci E, Ileri L. Analytical determination of contact stresses in mechanically fastened composites with finite boundaries. Int J Solids Struct 1993;30(18):2469–84.
[6] Hyer MW, Klang EC. Contact stresses in pin-loaded orthotropic plates. Int J Solids Struct 1985;21(9):957–75.
[7] Ireman T, Nyman T, Hellbom K. On design methods for bolted joints in composite aircraft structures. Compos Struct 1982;25:567–78.
[8] Chang FK, Scott RA, Springer GS. Strength of mechanically fastened composite joints. J Compos Mater 1982;16:470–94.

[9] Othieno M. Stress and failure analysis of composite pin loaded joints. Ph.D. Thesis, Howard University; 2000.
[10] Zhang K, Ueng CES. Stresses around a pin-loaded hole in orthotropic plates. J Compos Mater 1994;18:432–46.
[11] Whitworth HA, Othieno M, Barton O. Failure analysis of composite pin loaded joints. Compos Struct 2003;59:261–6.
[12] Tan SC. Mechanical response and design of notched composite laminates filled with reinforcement. J Compos Mater 1991;10:557–83.
[13] Konish HJ, Whitney JM. Approximate stress as in an orthotropic plate containing a circular hole. J Compos Mater 1975;9:157–66.
[14] Whitney JM, Nuismer RJ. Stress fracture criteria for laminated composites containing stress concentrations. J Mater 1971;5:253–65.
[15] Yamada SE, Sun CT. Analysis of laminate strength and its distribution. J Compos Mater 1978;12:275–84.
[16] Tan SC. Finite-width correction factors for anisotropic plate containing a central opening. J Compos Mater 1988;22:1080–97.
[17] Lessard LB, Poon C, Fahr A. Composite pinned joint failure modes under progressive damage. In: ECCM-V, 5th European conference on composite materials, Bordaeux, France; 1992. p. 49–54.